

Article

Effects of liquefaction temperature and time on characterization of liquefied oil palm trunk residue in the presence of polyhydric alcohols

Rattana Choowang, Jian LIN*, Guangjie ZHAO

Beijing Key Laboratory of Wood Science and Engineering, Beijing Forestry University, Beijing, 100083, P. R. China;

* Correspondence: linjian0702@bjfu.edu.cn; Tel.: +86-010-62336907

Abstract: Residues derived from liquefaction of oil palm trunk in the presence of polyhydric alcohol with different liquefaction temperature and time were characterized to provide a new approach to understand some fundamental aspects of the liquefaction reaction. Higher temperature and longer reaction time resulted in lower residue content, indicating more decomposition of components of oil palm trunk. The amorphous polymer comprised of lignin, hemicellulose, starch, and cellulose with non-crystalline structure are firstly degraded at low liquefaction temperature, followed by the decomposition of crystalline region of cellulose. Although it was relatively difficult to destroy the ordered structure of cellulose, most of them could be liquefied via prolonging reaction time or enhancing reaction temperature. Nevertheless, it was found that re-condensation of liquefied products occurred during the liquefaction process when higher temperature of 180 °C was used after 60 min, leading to the gradual increase of residue content with increase of reaction time.

Keywords: Oil palm; Liquefaction; Residue; Polyhydric alcohols

1. Introduction

As one of the main agricultural waste, the oil palm trunk biomass can be annually harvested from replanted palm plantation with the total amount of around 95 million tons, providing a continuous supply for the oil palm biomass industry [1]. However, few utilization of this biomass was conducted except for medium density fiberboard, fertilizer, molded wares, pulp and paper. A more valuable application such as cellulose nanocrystals has also been developed [2-3]. Most of them were almost left to rot in the field without utilization. Considering the content of chemical compositions, oil palm trunk is suitable for preparing the liquefied product which could be used to produce the carbon fibers and further activated carbon fibers [4-6]. Comparatively, it seems to be a more promising process for converting the oil palm trunk into high value-added materials.

Generally, both phenol and polyhydric alcohols have been used as liquefying solvent for the liquefaction of several lignocellulose materials with the catalysts of mineral or organic acids at a certain temperature for various time [7-9]. In the case of phenol, it possesses excellent solvolysis ability towards lignocellulose with consequent phenolation and dehydration of each composition part, leading to more formation of various phenolated compounds [10]. Considering environmental protection issues and liquefaction cost, liquefying solvent of polyhydric alcohols exhibits more advantages than those of phenol, resulting in more and more focus on it.

Previously, several type of polyhydric alcohols have been investigated. It was found that the ethylene carbonate (EC) gave higher percentage of liquefied yields than that of ethylene glycol (EG)

in the case of the liquefied bamboo process under 5% of hydrochloric as a catalyst and liquefaction temperature at 180 °C, attributing to their different dielectric constant values [10]. Besides, polyethylene glycol (PEG) showed higher liquefied rate of biomass than EG and EC, respectively, within 40 min of liquefaction [11]. However, the re-condensation occurred during the liquefaction process when applying the PEG alone, leading to low yield liquefied product. This results are corresponded to the previous report [12]. Fortunately, the liquefied yield can be enhanced by adding proper proportion of glycerol in PEG. The resultant mixture of PEG and glycerol exhibited excellent liquefying ability and have been applied in liquefaction process for various biomass such as corn starch, bagasse, cotton, bamboo, wheat straw, corncob, and others [13-16].

Furthermore, most previous researches concerning the liquefaction in the presence of polyhydric alcohol focused on the liquefaction fragments, but paid few attention about residue which is usually an evaluation of the extent of a liquefaction reaction. It is significantly to characterize the liquefied residue so as to better understand the liquefaction process. Accordingly, in this article we describe the efforts directed at the characterization and evaluation of liquefied residues derived from the liquefaction of oil palm trunk in the mixture of PEG and glycerol with various reaction temperature and time.

2. Materials and Methods

2.1. Materials

Oil palm trunks were harvested from a replantation for 30 years old in Surat Thani province in Southern of Thailand. Those trunks were felled at 60 cm from ground and cut into 1 meter length of logs. The logs were sawn into lumbers and then cut into chips by using a chipper and dried in hot air oven at 60 °C to reduce a moisture content. The dried chips were ground into fine powders that pass through screen size (200 mesh) with a Willey Mill. The fine powders were kept in desiccator until used. PEG-400 and glycerol as well as sulfuric acid were purchased from SINOPHARM group Chemical Reagent Co., Ltd and used as received.

2.2. Liquefaction process

The PEG-400 was mixed with glycerol with the weight ratio of 4:1 to prepare liquefaction solvent. The oil palm trunk powders were placed in a round bottom flask together with the mixture of liquefaction solvent and 98 % aqueous sulfuric acid (2 % on the amount of liquefaction solvent) at the weight ratio of 1:3. The flask was set up with magnetic stirrer and thermometer as well as reflux condenser system, and then immersed in an oil bath that was preheated at a various target temperatures from 130 °C to 180 °C for various reaction time from 30 to 120 min, respectively. After the reaction time, the flask was immersed in a cold water bath to stop reaction, and then 80 % 1, 4-dioxane aqueous solution was added to the reaction mixture. The resultant solution was filtrated through the filter paper which has been oven-dried and weighted before used. The insoluble liquefied residues after filtration were collected and dried in an oven at 103 °C until weight constant. The percentage of liquefied residue (LR) was calculated by following equation:

$$LR (\%) = (W_r / W_o) \times 100 \quad (1)$$

Where W_r is the oven-dried weight of the obtained liquefied residue after filtration (g), and W_o is the weight of oil palm trunk powder (g).

2.3. Chemical analyses

The chemical composition of used oil palm trunk consists of ash, extractive, Klason lignin, holocellulose and alpha cellulose were analyzed in accordance with Chinese's standard of GB/T 742-2008, GB/T 10741-2008, GB/T 10337-2008, GB/G 2677.10-1995 and GB/T 744-1989, respectively. Measurements of each component were conducted in at least triplicate, and the recorded data were found to be reproducible.

2.4. X-ray diffraction analysis

The crystalline of each liquefied residue were investigated by using X-ray diffraction apparatus (Smart lab, Japan) equipped with Ni-filtered Cu-K α radiation (wavelength of 1.5406 nm), the operating voltage of 40 kV and current of 40 mA. The intensities scanning was recorded between 5 ° to 50 ° (2 θ angle range) with a scan speed of 0.5 °/min and a scan step of 0.02 °. The crystallinity index value (CrI) of each obtained liquefied residues was calculated according to the Segal method per the following equation [17]:

$$\text{CrI} = (I_{002} - I_{\text{am}}) / I_{002} * 100 \quad (2)$$

Where I_{002} is the intensity of the diffraction from the (002) plane, and I_{am} is the intensity of the amorphous faction.

2.5. Solid state ^{13}C NMR spectroscopy

Solid state ^{13}C NMR spectroscopy (JNM-ECZ600R) equipped with a 3.2 mm probe was used for analyzing the liquefied residue. All experiments were conducted at frequencies of 100.55 MHz in a double-resonance MAS probehead at spinning speeds of 15 kHz and relaxation time of 2 ms as well as the pulse width of 6.5 μs . Each specimen was operated for 1 h at a temperature of 298 K.

2.6. Fourier transform infrared (FTIR) spectroscopy

The chemical functional groups of each liquefied residue were determined by using FTIR spectrometer with GX FT-IR system (PerkinElmer, Norwalk, CA, USA) in the scanning range of 4000 cm^{-1} to 400 cm^{-1} . The 1 mg of obtained liquefied residue powder was mixed with 99 mg of finely ground potassium bromide before building up a disk.

3. Results

3.1. Residue content

The liquefaction processes of oil palm trunk in the presence of the mixture of PEG-400 and glycerol were successfully conducted at various reaction temperature and time, respectively. The corresponding liquefied residues were obtained and the residue contents were calculated as shown in Figure 1. The residue content exhibited decreasing trends with increasing the liquefaction temperature from 130 °C to 180 °C regardless of the reaction time, indicating that the liquefied reaction can be accelerated by increasing the liquefaction temperature. For 30 min, around 50 %

decrease of residue content was obtained from 130 °C to 140 °C as similar as in terms of changing the liquefaction temperature from 170 °C to 180 °C. This might be caused by the decomposition of much amount of amorphous carbohydrate compounds in oil palm trunk such as hemicellulose and starch, which were easily transformed into small molecular under the heating and acid conditions. In addition, the liquefaction temperature at 140 °C gave the less liquefied residue content than heating with 150 °C. This may be due to the rapid degradation of oil palm in an acidic liquefaction solution, and then re-condensation among themselves. Besides, the re-condensation of liquefied products could be decomposed again depending on the temperature, time and acidity condition of solvent [18-19].

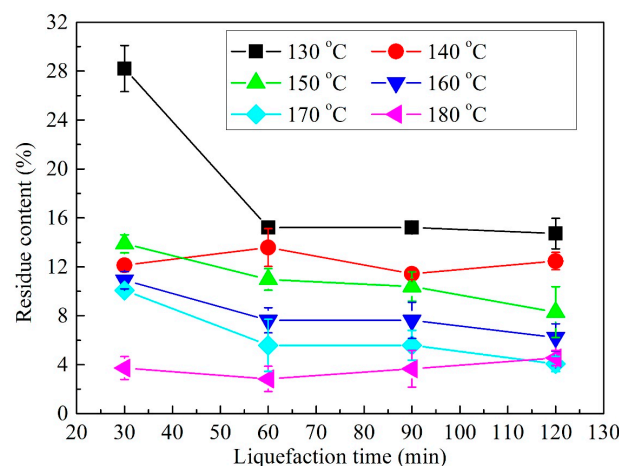


Figure.1. The residue content of liquefied oil palm trunk in presence of the mixture of PEG-400 and glycerol (80/20 w/w) at various reaction temperature and time.

However, it was not strongly affected on the acceleration of reaction rate of liquefaction when the reaction time were more than 30 min. Minor decrease in residue contents were obtained with increasing the liquefaction temperatures, attributing to the existing of around 11.3 % of cellulose in oil palm trunk. Cellulose possesses crystalline region and its molecular structure is orderly arranged so that the liquefaction solvent was difficult to penetrate into its structure. These results was also agreed with the previous report [20].

Additionally, the residue contents were almost dropped with the increase of reaction time except for the residue produced at the reaction temperature of 180 °C. It decreased from 3.7 % to 2.8 % when the reaction time increased from 30 min to 60 min at 180 °C, and then increased with the time prolonging. This means that the lowest residue content was obtained when the liquefaction time was 60 min, and it is nearly equally to the ash content of oil palm trunk of 2.7 %. Accordingly, all the main chemical components of oil palm trunk were almost liquefied into small fraction which then polymerized to form the residue, leading to approximately 60 % increase of residue content obtained for the reaction time of 120 min.

3.2. FTIR spectroscopy

FTIR has been proved to be an extremely useful method to investigate the chemical function groups of polymers. Figure. 2 illustrated the FTIR spectra of oil palm trunk and its residue after

liquefaction with different temperatures at 30 min. In spectrum of oil palm, the presence of band centered at around 3410 cm^{-1} was assigned to the stretching vibration of hydroxyl groups which were mainly derived from carbohydrate polymers such as starch, hemicellulose and cellulose, since the lower lignin content of 5.1 % in oil palm trunk [21]. After liquefaction, the broad peak was transformed into sharp one, and the bands shifted to the higher wavenumber of 3431 cm^{-1} upon all residues after different liquefaction time, indicating the decomposition of starch and then cleavage of hydrogen bonds being formed among the main chemical composition of oil palm trunk [22-23]. With the liquefaction temperatures increasing, it is observed that the skeletal mode vibration of the pyranose ring at the wavenumber of 576 cm^{-1} and C-H stretching vibration at 2930 cm^{-1} slightly decreased, which may be due to the decomposition of amorphous starch. When the liquefaction temperature of $180\text{ }^{\circ}\text{C}$, the peak of 576 cm^{-1} was almost disappeared. This may be indicative of the decomposition of all amorphous carbohydrate polymers and most of cellulose, leading to the lower residue content of 3.7 %.

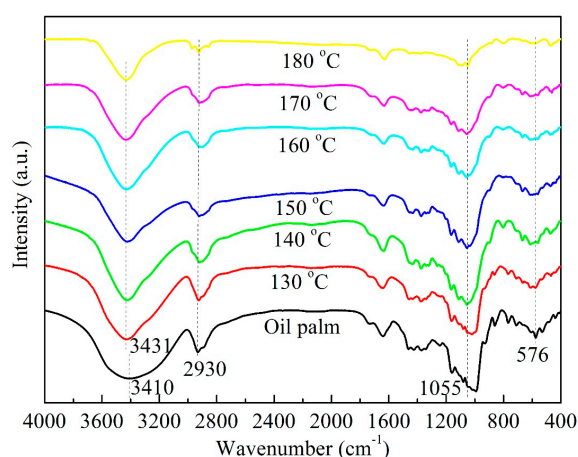


Figure.2. FTIR spectra of oil palm trunk and its residue after liquefaction with different temperatures at 30 min.

FTIR spectra of residues after liquefaction with different time at $170\text{ }^{\circ}\text{C}$ were obtained as shown in Figure. 3. Compared with raw material, the residue from liquefaction time of 30 min exhibited relatively sharp peak of 3431 cm^{-1} with higher wavenumber, due to the decomposition of starch. The peak at around 1055 cm^{-1} represented the ether bonds sharply became weak until the liquefaction time of 60 min, attributing to decomposition of non-crystalline cellulose, leading to the decrease of residue content from 10.1 % to 5.6 % [21]. When prolonging liquefaction time to 120 min, all the peaks obviously became weak. This may be the result of the fracture of crystalline region in cellulose. It can be also proved by the gradually weak peaks at 576 cm^{-1} and 2930 cm^{-1} , respectively. However, different phenomenon occurred in the residue after the liquefaction of $180\text{ }^{\circ}\text{C}$ as presented in Figure. 4. Almost all the chemical components were decomposed when the liquefaction time of 60 min, which is shorter than the liquefaction at $170\text{ }^{\circ}\text{C}$. The peak at 1055 cm^{-1} could be obviously observed after 60 min, which may be caused by the polymerization of liquefied products at higher temperature and formation of residue. That is why the residue content increased from liquefaction time of 60 min to 120 min. The above results can be further confirmed by NMR measurements.

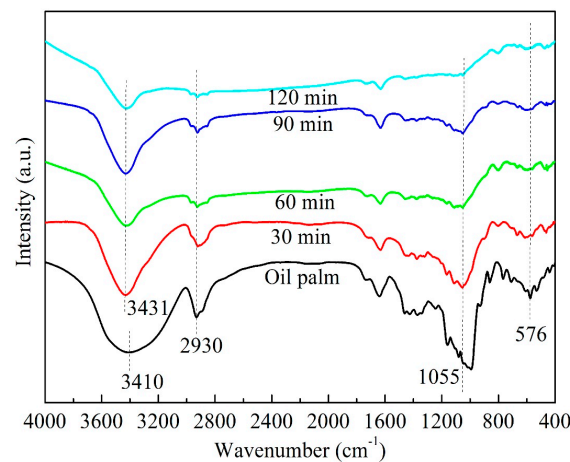


Figure.3. FTIR spectra of oil palm trunk and its residue after liquefaction with different time at 170 °C.

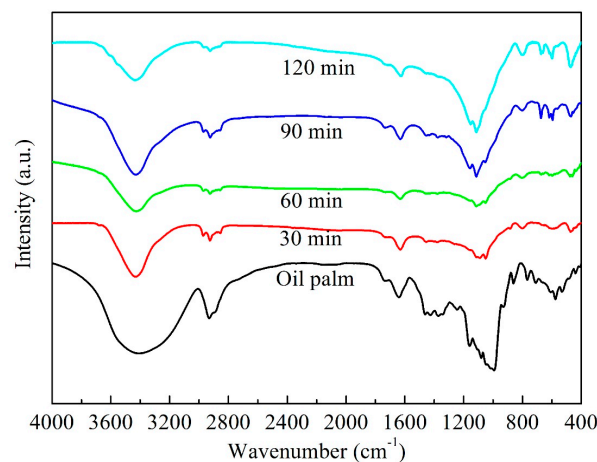


Figure.4. FTIR spectra of oil palm trunk and its residue after liquefaction with different time at 180 °C.

3.3. ^{13}C NMR analysis

The solid-state ^{13}C NMR of oil palm trunk and its residue with different liquefaction temperatures at 30 min were conducted and the corresponding spectra were shown in Figure. 5. The pattern of signals that obtained from oil palm raw material showed the main peak at 73.5 which is related to C2, C3 and C5 carbon in pyranose ring. The signals of 63.1 ppm and 85.5 ppm are demonstrated C6 and C4 carbon of the non-crystalline region, respectively [24]. While the signals in range of 102.5 to 106.6 ppm are agreed with C1, they are detected from the combination between α and β of C1 carbon in structure of starch and cellulose, respectively. The C6 carbon of crystalline region can usually be detected at 66.2 ppm, but it is represented very tiny peak for oil palm raw material. However, this peak can be clearly seen after the liquefaction with temperature at 140 °C as same as the C1 carbon of crystalline region was observed at 106.6 ppm because it loss α form of C1 carbon of starch (102.5 ppm), which can be detected at a lower signals than β form of cellulose [25].

The C4 carbon of crystalline region that was detected at 90.1 ppm appeared clearly after liquefaction. In contrast, the C6 carbon of the non-crystalline region (-CH₂OH) at 63.1 are continuously dropped when increased the liquefaction temperature from 130 °C to 180 °C. The signals that indicates the crystalline region comprised of 66.2 ppm (C6), 90.1 (C4) ppm and 106.6 ppm (C1), were remained slightly in term of 180 °C for 30 min. Therefore, it can be concluded that most amorphous carbohydrates (hemicellulose and starch as well as amorphous region of cellulose) were degraded by liquefaction at 140 °C for 30 min. The crystalline region were almost destroyed at high temperature of 180 °C for reaction time of 30 min.

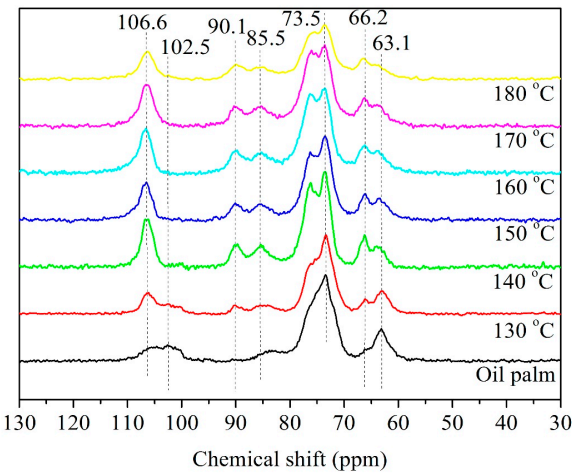


Figure.5. Solid state ¹³C NMR spectroscopy of oil palm trunk and its residue after liquefaction with different temperatures at 30 min.

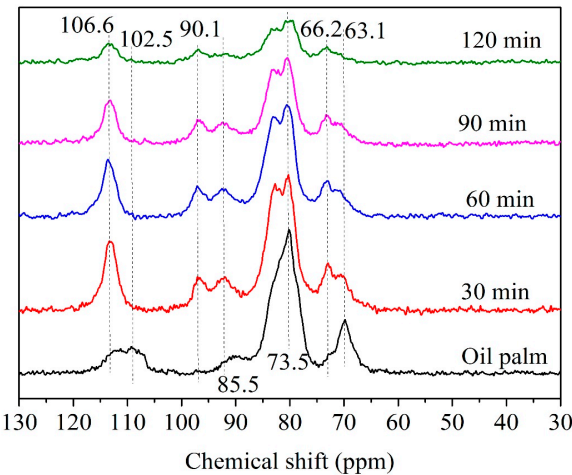


Figure.6. Solid state ¹³C NMR spectroscopy of oil palm trunk and its residue after liquefaction with different time at 170 °C.

The measurements of solid state ¹³C NMR of residue after liquefaction with different time at 170 °C were performed and the corresponding spectra were shown in Figure. 6. The signals of 63.1 ppm

and 85.5 ppm represented for C6 and C4 carbon of the non-crystalline region, respectively, were gradually weak, and the signal of 102.5 ppm for α C1 carbon in structure of starch could not be detected after 30 min of liquefaction, indicating the decomposition of amorphous starch and cellulose. These just made the increase of relative content of crystalline cellulose, which was also improved by the increase of intensity for the peaks of 66.2 ppm and 102.5 ppm. With the liquefaction time increasing, the peaks of crystalline cellulose became weak, illustrating that more and more cellulose were destroyed.

3.4. X-ray diffraction analysis

The chemical components of oil palm trunk were liquefied at various temperatures as a result of the different contents of crystalline structures existing in resultant residues. The X-ray diffractogram patterns of oil palm trunk and resultant residues obtained from the temperatures of 130 °C to 180 °C for 30 min were presented in Figure. 7. From the pattern of oil palm, the typical peaks at 2θ value of 15.2 ° and 22.8 ° attributed to the (110) and (002) crystallographic plane, respectively, could be observed, indicating the crystalline structure in cellulose I [3, 26-28].

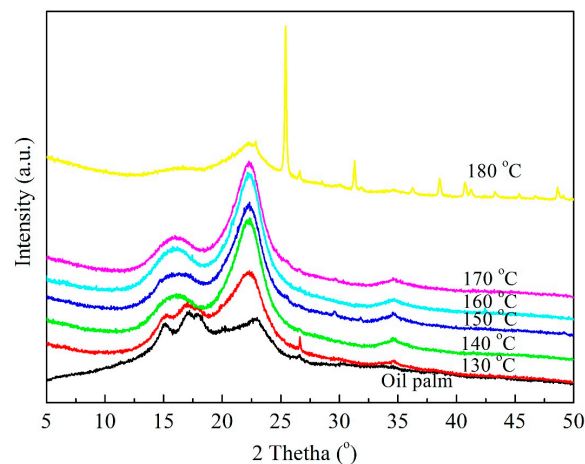


Figure.7. X-ray diffraction patterns of oil palm trunk and its residue after liquefaction with different temperatures at 30 min.

With increasing the reaction temperatures from 130 °C to 170 °C, the peaks at 2θ value of 22.8 ° became narrower and sharper, indicating that the intensity of 002 crystallographic plane are relatively increasing. Thus, the corresponding crystallinity index was found to be 51.7 %, 74.0 %, 73.0 %, 75.5 %, and 78.4 %, respectively, which are extremely higher than that of oil palm of 21.1 %. These may be due to the decomposition of a large amount of amorphous structure, especially for amylose [29-30]. Whilst much crystalline region were destroyed within 30 min under high temperature of 180 °C according to the peak at 2θ value of 22.8 ° with relatively low intensity. The degradation of crystalline regions was promoted by the organic acids such as acetic acid and formic acid as well as levulinic acid, which were derived from degraded chemical components during liquefaction reaction at high temperature [31-32]. Besides, one sharp and strong peak at 2θ around 25.4 ° accompanied with other small peaks at higher 2θ can be obviously observed in the X-ray

diffraction pattern of resultant residue from liquefaction at 180 °C. These peaks were related to a crystalline silica which is the main component of ash in oil palm trunk.

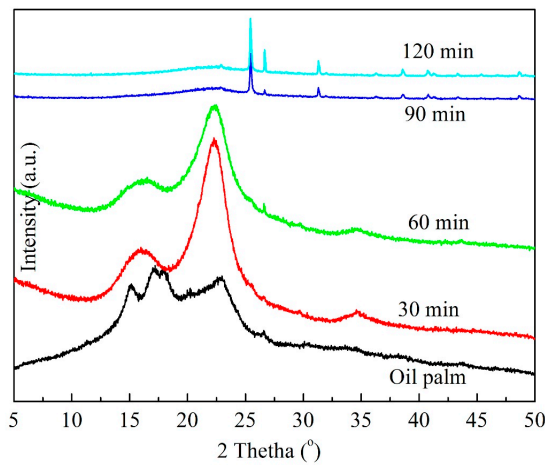


Figure.8. X-ray diffraction patterns of oil palm trunk and its residue after liquefaction with different time at 170 °C.

The X-ray diffraction of residue derived from the liquefaction with different time from 30 min to 120 min at 170 °C were determined as presented in Figure. 8. Compared with the oil palm, residues exhibited completely different patterns. With the liquefaction time increasing, the peak at 2θ value of 22.8 ° firstly became sharper and then gradually smaller because of the decomposition of cellulose, leading to the decrease of crystallinity index ranging from 78.4 % to 35.7 %. Weaker and broader peak could be obviously observed after the liquefaction time of 90 min. Besides, the peaks at 2θ value of 15.2 ° in all patterns were gradually weak and disappeared when 90 min and 120 min, indicating that the crystalline region in cellulose were almost destroyed. These results are greatly agreed with the above measurements of FITR and NMR.

4. Conclusions

Liquefaction of oil palm trunk were successfully performed with polyhydric alcohols under various temperature and time, and the corresponding residues were investigated. With the liquefaction temperature increasing, the degradation of most amorphous carbohydrates such as hemicellulose and starch as well as amorphous region of cellulose occurred, leading to the gradual increase of crystallinity index from 21.1 % to 78.4 % and obvious decrease of resultant residue content. When the crystalline region were almost destroyed at high temperature of 180 °C, the residue content lowed to around 4 %. Besides, longer liquefaction time engendered more adequate liquefaction of each component in oil palm trunk for the liquefaction temperature from 130 °C to 170 °C, resulting in the decrease of residue content. While the residue content increased after 60 min of liquefaction at 180 °C, mainly attributing to the re-condensation of liquefied products.

Acknowledgments: This research was financially supported by “Beijing Municipal Education Commission Co-building Project of Scientific Research and Postgraduate Training for Key Disciplines (2015)” and “The National Natural Science Foundation of China (No.31700492)”, which are gratefully acknowledged.

Author Contributions: Rattana Choowang did the experiments, data analysis and wrote the draft; Jian Lin and Guangjie Zhao reviewed and revised the draft.

Conflicts of Interest: The authors declare no conflict of interest.

References

1. Lamaming, J.; Hashim, R.; Sulaiman, O.; Leh, C.P.; Sugimoto, T.; Nordin, N.A. Cellulose nanocrystals isolated from oil palm trunk. *CARBOHYD. POLYM.* **2015**, *127*, 202-208, DOI: <https://doi.org/10.1016/j.carbpol.2015.03.043>.
2. Mohamad Haafiz, M.K.; Eichhorn, S.J.; Hassan, A.; Jawaid, M. Isolation and characterization of microcrystalline cellulose from oil palm biomass residue. *CARBOHYD. POLYM.* **2013**, *93*, 628-634, DOI: <https://doi.org/10.1016/j.carbpol.2013.01.035>.
3. Lamaming, J.; Hashim, R.; Sulaiman, O.; Leh, C.P.; Sulaiman, O. Properties of cellulose nanocrystals from oil palm trunk isolated by total chlorine free method. *CARBOHYD. POLYM.* **2017**, *156*, 409-416, DOI: <https://doi.org/10.1016/j.carbpol.2016.09.053>.
4. Ma, X.J.; Zhao, G.J. Preparation of carbon fibers from liquefied wood. *WOOD SCI. TECHNOL.* **2010**, *44*, 3-11, DOI: <https://doi.org/10.1007/s00226-009-0264-3>.
5. Hashim, R.; Nadhari, W.N.A.W.; Sulaiman, O.; Kawamura, F.; Hiziroglu, S.; Sato, M.; Sugimoto, T.; Seng, T.G.; Tanaka, R. Characterization of raw materials and manufactured binderless particleboard from oil palm biomass. *MATER. DESIGN.* **2011**, *32*, 246-254, DOI: <https://doi.org/10.1016/j.matdes.2010.05.059>.
6. Liu, W.J.; Zhao, G.J. Effect of temperature and time on microstructure and surface functional groups of activated carbon fibers prepared from liquefied wood. *BioResources* **2012**, *7*(4), 5552-5567.
7. Alma, M.H.; Yoshioka, M.; Yao, Y.; Shiraishi, N. Preparation of sulfuric acid-catalyzed phenolated wood resin. *WOOD SCI. TECHNOL.* **1998**, *32*, 297-308, DOI: <https://doi.org/10.1007/BF00702897>.
8. Zhang, Y.; Ikeda, A.; Hori, N.; Takemura, A.; One, H.; Yamada, T. Characterization of liquefied product from cellulose with phenol in the presence of sulfuric acid. *BIORESOURCE TECHNOL.* **2006**, *97*, 313-321, DOI: <https://doi.org/10.1016/j.biortech.2005.02.019>.
9. Pan, H. Synthesis of polymers from organic solvent liquefied biomass: A review. *RENEW. SUST. ENERG. REV.* **2011**, *15*, 3454-3463, DOI: <https://doi.org/10.1016/j.rser.2011.05.002>.
10. Yip, J.; Chen, M.J.; Szeto, Y.S.; Yan, S.C. Comparative study of liquefaction process and liquefied products from bamboo using different organic solvents. *BIORESOURCE TECHNOL.* **2009**, *100*, 6674-6678, DOI: <https://doi.org/10.1016/j.biortech.2009.07.045>.
11. Guo, Z.H.; Liu, Y.N.; Wang, F.Y.; Xiao, X.Y. Liquefaction of metal-contaminated giant reed biomass in acidified ethylene glycol system: Batch experiments. *J. CENT. SOUTH. UNIV.* **2014**, *21*, 1756-1762, DOI: <https://doi.org/10.1007/s11771-014-2121-2>.
12. Yamada, T.; Hu, Y.; Ono, H. Condensation reaction of degraded lignocellulose during wood liquefaction in the presence of polyhydric alcohols. *J. ADHES. SOC. JAPAN* **2001**, *37*(12), 471-478, DOI: 10.11618/adhesion.37.471.
13. Yao, Y.; Yoshioka, M.; Shiraishi, N. Water-absorbing polyurethane foams from liquefied starch. *J. APPL. POLYM. SCI.* **1996**, *60*, 1939-1949, DOI: 10.1002/app.1097-4628.
14. Chen, F.; Lu, Z. Liquefaction of wheat straw and preparation of rigid polyurethane foam from the liquefaction products. *J. APPL. POLYM. SCI.* **2009**, *111*, 508-516, DOI: 10.1002/app.29107.
15. Zhang, H.; Luo, J.; Li, Y.; Guo, H.; Xiong, L.; Chen, X. Acid-catalyzed liquefaction of bagasse in the presence of polyhydric alcohol. *APPL. BIOCHEM. BIOTECH.* **2013**, *170* (7), 1780-1791, DOI: <https://doi.org/10.1007/s12010-013-0300-5>.
16. Zhang, H.; Pang, H.; Shi, J.; Fu, T.; Liao, B. Investigation of liquefied wood residues based on cellulose, hemicellulose, and lignin. *J. APPL. POLYM. SCI.* **2012**, *123*, 850-856, DOI: 10.1002/app.34521.
17. Segal, L.; Creely, J.J.; Martin, A.E.; Conrad, C.M. An empirical method for estimating the degree of crystallinity of native cellulose using the x-ray diffractometer. *TEXT. RES. J.* **1959**, *29*, 786-794, DOI: <https://doi.org/10.1177/004051755902901003>.
18. Hoover, R. Acid-treated starches. *FOOD REV. INT.* **2000**, *16*, 369-392, DOI: <https://doi.org/10.1081/FRI-100100292>.
19. Kobayashi, M.; Asano, T.; Kajiyama, M.; Tomita, B. Analysis on residue formation during wood liquefaction with polyhydric alcohol. *J. Wood SCI.* **2004**, *50*, 407-414, DOI: <https://doi.org/10.1007/s10086-003-0596-9>.

20. Kim, K.H.; Yu, J.H.; Lee, E.Y. Crude glycerol-mediated liquefaction of saccharification residues of sunflower stalks for production of lignin biopolyols. *J. IND. ENG. CHEM.* **2016**, *38*, 175-180, DOI: <https://doi.org/10.1016/j.jiec.2016.05.002>.
21. Silverstein, R.M.; Webster, F.X.; Kiemle, D.J. Infrared Spectrometry. In *Spectrometric identification of organic compounds*, 7th ed.; John Wiley & Sons, Inc.: 111 River Street, Hoboken, NJ 07030-5774, United States of America, 2005; pp. 72-126, ISBN 0-471-39362-2.
22. Kaddla, J.F.; Kubo, S. Lignin-based polymer blends: Analysis of intermolecular interactions in lignin-synthetic polymer blends. *COMPOS. PART A-APPL. S.* **2004**, *35*, 395-400, DOI: <https://doi.org/10.1016/j.compositesa.2003.09.019>.
23. Kubo, S.; Kadla, J.F. Hydrogen bonding in lignin: A Fourier transform infrared model compound study. *Biomacromolecules*, **2005**, *6*, 2815-2821, DOI: [10.1021/bm050288q](https://doi.org/10.1021/bm050288q).
24. Wi, S. G.; Cho, E.J.; Lee, D.S.; Lee, S.J.; Lee, Y.J; Bae, H.J. Lignocellulose conversion for biofuel: a new pretreatment greatly improves downstream biocatalytic hydrolysis of various lignocellulosic materials. *BIOTECHNOL. BIOFUELS.* **2015**, *8*, 228-238, DOI: [10.1186/s13068-015-0419-4](https://doi.org/10.1186/s13068-015-0419-4).
25. Chen, Y.Y.; Luo, S.Y.; Hung, S.C.; Chan, S.I.; Tzou, D.L.M. ¹³C Solid-state NMR chemical shift anisotropy analysis of the anomeric carbon in carbohydrates. *CARBOHYD. RES.* **2005**, *340*, 723-729, DOI: <https://doi.org/10.1016/j.carres.2005.01.018>.
26. Wada, M.; Okano, T.; Sugiyama, J. Allomorphs of native crystalline cellulose I evaluated by two equatorial d-spacings. *J. WOOD SCI.* **2001**, *47*, 124-128, DOI: <https://doi.org/10.1007/BF00780560>.
27. Popescu, M.C.; Popescu, C.M.; Lisa, G.; Sakata, Y. Evaluation of morphological and chemical aspects of different wood species by spectroscopy and thermal methods. *J. MOL. STRUCT.* **2011**, *988*, 65-72, DOI: <https://doi.org/10.1016/j.molstruc.2010.12.004>.
28. Poletto, M.; Zattera, A.J.; Forte, M.M.C.; Santana, R.M.C. Thermal decomposition of wood: influence of wood components and cellulose crystallite size. *BIORESOURCE TECHNOL.* **2012**, *109*, 148-153, DOI: [10.1016/j.biortech.2011.11.122](https://doi.org/10.1016/j.biortech.2011.11.122).
29. Atichokudomchai, N.; Shobsngob, S.; Chinochoti, P.; Varavinit, S. A study of some physicochemical properties of high-crystalline tapioca starch. *Starch-Stärke* **2015**, *53*, 577-581.
30. Wang, Q.; Chen, Q.; Qiao, Q.; Sugiyama, K.; Wang, Q.Y. Process analysis of the waste bamboo by using polyethylene glycol solvent liquefaction. *INTER. J. SUS. DEVELOP. PLAN.* **2014**, *9*, 647-657, DOI: [10.2495/SDP-V9-N5-647-657](https://doi.org/10.2495/SDP-V9-N5-647-657).
31. Yamada, T.; Ono, H. Characterization of the products resulting from ethylene glycol liquefaction of cellulose. *J. WOOD SCI.* **2001**, *47*, 458-464, DOI: <https://doi.org/10.1007/BF00767898>.
32. Rezzoug, S.A.; Capart, R. Liquefaction of wood in two successive steps: solvolysis in ethylene-glycol and catalytic hydrotreatment. *APPL. ENERG.* **2002**, *72*, 631-644, DOI: [https://doi.org/10.1016/S0306-2619\(02\)00054-5](https://doi.org/10.1016/S0306-2619(02)00054-5).